ISSN: 1001-4055 Vol. 45 No. 2 (2024)

Pore Diameter and Carbon Composition of Walnut Shells of Tidore Islands, North Maluku, Indonesia

I Dewe K. Anom¹, Marianus², J. Z. Lombok¹, Saprizal Hadisaputra³, I Dewa Gede Katja⁴ and J. J. Mamangkey⁵

¹Department of Chemistry, Faculty of Mathematics and Natural Sciences Universitas Negeri Manado, Indonesia ²Department of Physics, Faculty of Mathematics and Natural Sciences Universitas Negeri Manado, Indonesia (marianus@unima.ac.id)

¹Department of Chemistry, Faculty of Mathematics and Natural Sciences Universitas Negeri Manado, Indonesia (johnylombok@unima.ac.id)

³Chemistry Education Division, Faculty of Teacher Training and Education, University of Mataram, Indonesia (rizal@unram.ac.id)

⁴Department of Chemistry, Faculty of Mathematics and Natural Sciences Sam Ratulangi University, Indonesia (dewakatja@unsrat.ac.id)

⁵Department of Biology, Faculty of Mathematics and Natural Sciences Universitas Negeri Manado, Indonesia (jefrimamangkey@unima.ac.id)

Corresponding Author: ideweketut@unima.ac.id

ABSTRACT

Walnut shell carbon was produced using the pyrolysis method at 350 °C. The pyrolyzed carbon was activated using 3M of KOH activator. The pyrolyzed and KOH-activated carbon were analyzed with FTIR, SEM-EDX, and XRD. The functional group identified from the KOH-activated carbon of the walnut shell is the aromatic C-H group, C-H aliphatics, C-O alcohol, C-O acetic acid, and C-O ester. The diameter of the pyrolyzed carbon pores is 333.9-2839 nm, while the KOH-activated one is 1217-2137 nm. The composition of the carbon elements increased from 70.6% (pyrolised carbon) to 79.40% (KOH-activated). Based on the results of the XRD analysis, both carbons show widening and amorphous peaks.

Keywords: Walnut Shell, Carbon, Pyrolysis, Carbon activation, FTIR, SEM, EDX, XRD.

INTRODUCTION

Walnut (*Canarium vulgare leenh*) is a native Indonesian plant that grows mostly in Eastern regions, such as Maluku and Tidore. Walnuts are very popular with consumers in Maluku because of their good taste. Maluku and Tidorean people like to consume walnuts that have not been dried. Walnuts are rich in saturated and unsaturated fatty acids. A walnut shell is a part of the walnut fruit not utilized by the community, is discarded as waste, and is considered to have no economic value. Walnut shells have a strong physical structure sufficient to be utilized as charcoal. In Indonesia, about 86 tons per year of walnut shells are not optimally utilized, some of which are only used as firewood, and the rest are thrown away. Walnut skin and shells are a major source of lignocellulose. However, walnut shell waste can be converted into activated carbon, a processed product of walnut shell pyrolysis. The chemical composition of the walnut shell consists of 39.24% cellulose, 38.00% lignin, 11.72% water, 9.25% hemicellulose, and 1.79% ash. The main products resulting from the pyrolysis of walnut shells are charcoal 36.80%, liquid smoke 42.58%, tar 4.48%, and 15.79% volatile noncondensable gas components. Their functional groups vary, namely hydroxy 3 groups (R-OH), carbonyl (R-C=O), esters (R-CO-O-R'), alkanes (R-CH₂), carboxyl (R-COOH) and aromatic groups (R-CH).

Charcoal is a porous material; tar, hydrocarbons, and other organic compounds cover most portions. Besides generating charcoal, this heating or decomposition process produces other products, such as liquids and gases. ^{8.9} Pyrolysis is the process of heating at a high or a predetermined temperature without oxygen, and activation uses

Tuijin Jishu/Journal of Propulsion Technology

ISSN: 1001-4055 Vol. 45 No. 2 (2024)

chemicals. ^{10,11,12} Activated carbon with high porosity and surface area can be obtained through hydroxy alkalis chemical processes. ^{13,14} Among the existing hydroxy alkalis (NaOH, LiOH, and KOH), KOH is the most effective activator that has been widely studied. ^{15,16} The activated carbon widely used as an absorbent material in industry. ^{15,17}.

In this study, walnut shells were taken from the mountains in Tidore Islands Regency. Walnut trees that grow in the mountains affect the composition of the elements that make up the walnut shell. The choice of KOH as an activator for the chemical activation process on carbon materials is considered very appropriate due to its strong base and hygroscopic properties. ^{18, 19} The chemical activation process is to activate walnut shell carbon by adding certain chemicals to the sample and increase the pore diameter so that the carbon pores are open. ^{20,21} After the carbonization process, the carbon is chemically activated with the help of chemical solutions such as acidic. ²² or basic compounds. ²³ Furthermore, walnut shell charcoal was characterized using instruments Fourier Transform Infrared (FTIR), Scanning Electron Microscope (SEM), Energy Dispersive X-ray (EDX), and X-ray Diffraction (XRD). XRD is used to obtain structural information and the character of walnut shell charcoal. XRD analysis can reveal significant changes in crystal size for samples carbonized at a wide temperature range (900-1500°C). ²⁴

EXPERIMENTAL

Tools and materials

The tools used were glassware, oven, furnace, porcelain cup, 100 mesh filter, FTIR, SEM-EDX, XRD. The materials used were walnut shells from the Tidore Islands district, North Maluku, Indonesia, 3M KOH, distilled water, filter paper and universal indicator.

Research procedure

The walnut shell samples were cleaned from the shells attached to the outside and dried in the sun to reduce the water content. The walnut shell samples were pyrolyzed in a pyrolysis reactor and heated to 350°C for 6 hours. The resulting charcoal or carbon was allowed to cool, and then it was ground using a mortar and sieved and filtered through a 100 mesh sieve. A fine filtered 20 g of walnut shell carbon was immersed in 100 mL of 3M KOH solution for 24 hours. The mixture was filtered using filter paper, then washed with distilled water until the washing solution became neutral at pH ±7. The residue was dried in an oven at 110-120 °C for 4 hours. After that, it was stored in a desiccator until the carbon stabilized. FTIR measurements using a Shimadzu type IRprestige-21 FTIR Spectrophotometer working at a scan range of 4000-340 cm-1, resolution of 4 cm-1, and scan of 2-3 seconds. Paired with an EDX device, SEM was used to examine the morphology and determine the relative carbon content or composition ²⁶. X-ray diffraction (XRD) analysis is the basic method to evaluate the structure of carbon arrays or determine the crystal structure. ^{17,27}

RESULTS AND DISCUSSION

FTIR Analysis

FTIR analysis determines the functional groups present and lost after carbon activation based on the absorption band pattern at the wavenumber. The FTIR characterization results of pyrolyzed (control) and KOH-activated walnut shell carbon are shown in Figure-1. The FTIR spectra of pyrolyzed and KOH-activated walnut shell carbon have almost the same absorption band pattern. A comparison of the two spectra showed that after KOH activated the carbon, there was a shift in the wavenumber from 3028.24 cm⁻¹ to 3068.75 cm⁻¹. Absorption intensity decreased at wavenumbers 1259.52 cm⁻¹ and 879.5 cm⁻¹, down to 1234.44 cm⁻¹ and 875.68 cm⁻¹. There is also new absorption of KOH-activated carbon wave numbers 2422.59 cm⁻¹, 1317.38 cm⁻¹, 1234.44 cm⁻¹, and 590.22 cm⁻¹. The loss of several absorption peaks and the decrease in absorption intensity indicate the reduction of impurities in carbon. It indicates the formation of aromatic compounds, constituents of the carbon structure.²⁸

Vol. 45 No. 2 (2024)

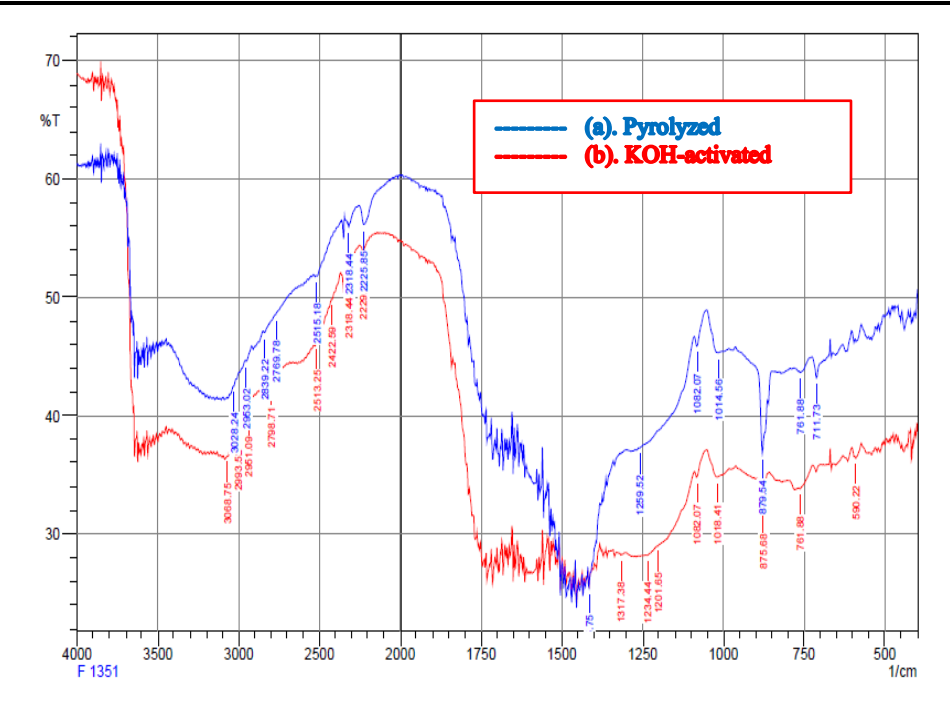


Fig.-1: FTIR Spectra of Pyrolyzed (a) and KOH-Activated Walnut Shell Carbon (b).

Absorption functional groups (seen Tabel 1), at wave numbers 3028.24 - 3068.75 cm⁻¹ indicates the presence of C-H functional groups in aromatic groups, followed by absorption at wave numbers 879.54-590.22 cm⁻¹, the vibration of secondary aromatic C-H groups.²⁹ The absorption at wave number 1317.38 cm⁻¹ shows the vibration of the C-O group of alcohol and carboxylic acid. Absorption at wave numbers 1259.52-1234.44 cm⁻¹ and 1082.07 cm⁻¹ show the presence of C-O ester functional groups. The absorption at wave numbers 879.54-875.68 cm⁻¹ and 761.88 cm⁻¹ show aromatic C-H vibrations.³⁰

Table-1: FTIR Spectra Absorption Bands of Pyrolyzed and KOH-Activated Walnut Shell Carbon.

Wave num	ber (cm ⁻¹)	Functional Group	
3028.24	3068.75	C-H aromatic	
2422.59	2422.59	C-H aliphatic	
1317.38	1317.38	C-O alcohol/carboxylic acid	
1259.52	1234.44	C-O ester	
1082.07	1082.07	C-O ester	
879.54	875.68	C-H aromatic	
761.88	761.88	C-H aromatic	
	590.22	C-H aromatic	

SURFACE MORPHOLOGY ANALYSIS OF WALNUT SHELL CARBON

The pyrolysis process of walnut shells is an important step in obtaining carbon as the final product. Pyrolysis is a heating process without oxygen that aims to carbonize and increase carbon content. The surface morphological structure of carbon from pyrolyzed walnut shell and carbon after KOH activation was analyzed by Scanning Electron Microscopy (SEM). The results of SEM analysis on pyrolyzed walnut shell carbon and carbon after KOH activation are shown in Figure-2. Figure-2 (a, b, c) shows the surface morphology of walnut shell carbon from pyrolysis and after KOH activation (d, e, f) with magnifications of 1000, 3000, and 5000, both of which have different pore surfaces that are non-uniform and irregular. The pyrolysis process and the addition of the KOH activator produce outer pores with non-uniform surfaces scattered throughout the carbon surface. ³¹ Adding

a KOH solution activator to walnut shell carbon aims to dissolve metal elements contained in carbon and increase carbon content. The activation process causes many volatile compounds to be released or vaporized, thus opening carbon pores and reducing hydrocarbon closure which is in accordance with what has been previously stated. 9,32 that the formation and enlargement of pores caused by the evaporation of degraded cellulose components. There needs to be more uniformity in the pore structure on the carbon surface, indicating the presence of organic impurities or tar that has not evaporated and covered some pores. 21,33

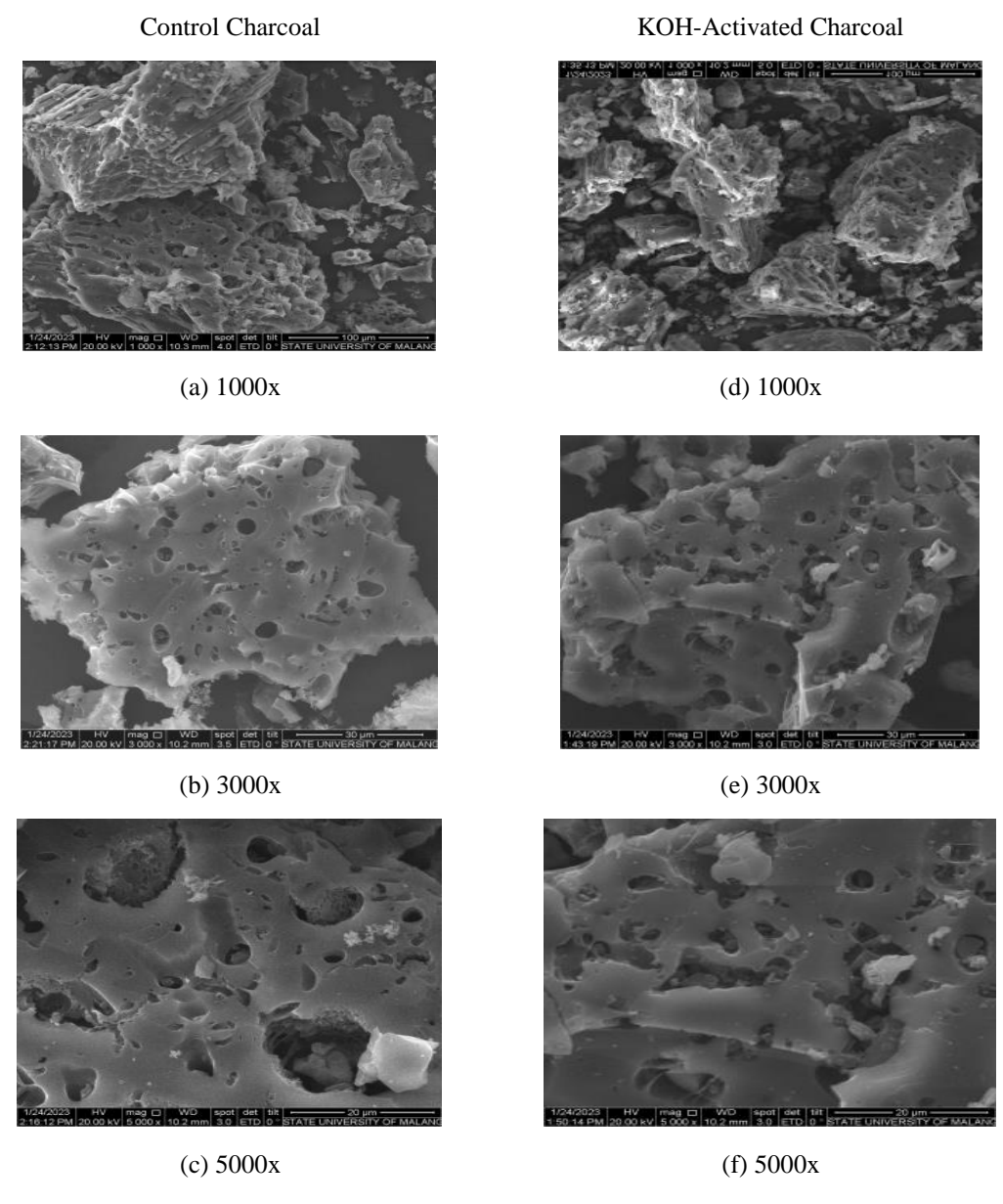


Fig.-2: SEM Surface Morphology of Pyrolyzed (a-c) and KOH-Activated (d-f) Walnut Shell Carbon With Magnification 1000, 3000, and 5000x.

Figure-3 shows the SEM morphology of pyrolyzed (a) and KOH-activated (b) walnut shell carbon with a magnification of 10,000x, respectively. It can be seen that the pore diameter of pyrolyzed and KOH-activated walnut shell carbon varies greatly. The pore diameters are not uniform (Table-2). The pore diameter of pyrolyzed walnut shell carbon ranges from 339.8 nm to 2,839 μm . In contrast, the pore diameter of KOH-activated walnut shell carbon ranges from 1,217 μm to 2,137 μm . The pore diameter of KOH-activated walnut shell carbon is larger than the pyrolyzed one, but the difference in pore diameter between one and the other is not too large. $\frac{28}{3}$

ISSN: 1001-4055 Vol. 45 No. 2 (2024)

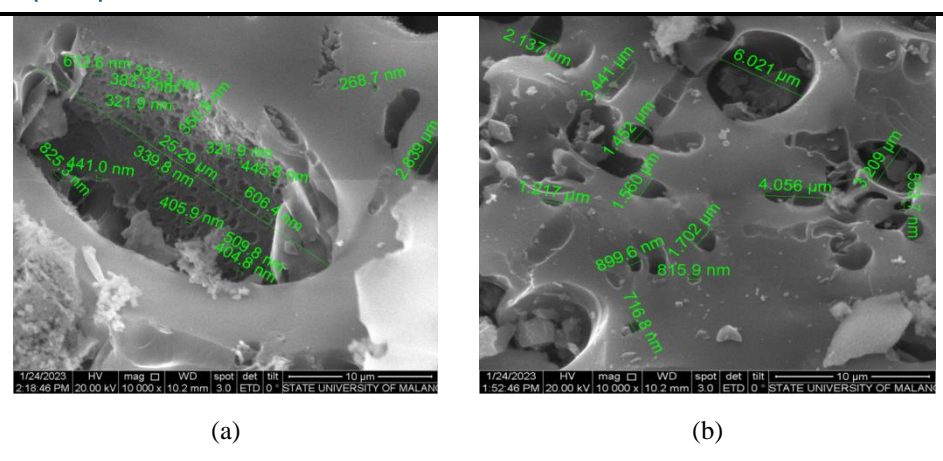


Fig.-3: SEM Morphology of Pyrolyzed (a) and KOH-Activated (b) Walnut Shell Carbon at 10,000x Magnification.

The results showed that these pores are macro pores.^{34,35}, with a pore diameter of over 50 nm. The non-uniformity of pore diameter is influenced by factors KOH activator³⁶ and contains other chemically bound elements such as oxygen and hydrogen.^{37,38,39}

Table 2: Pore Diameter of Pyrolyzed and KOH-Activated Walnut Shell Carbon.

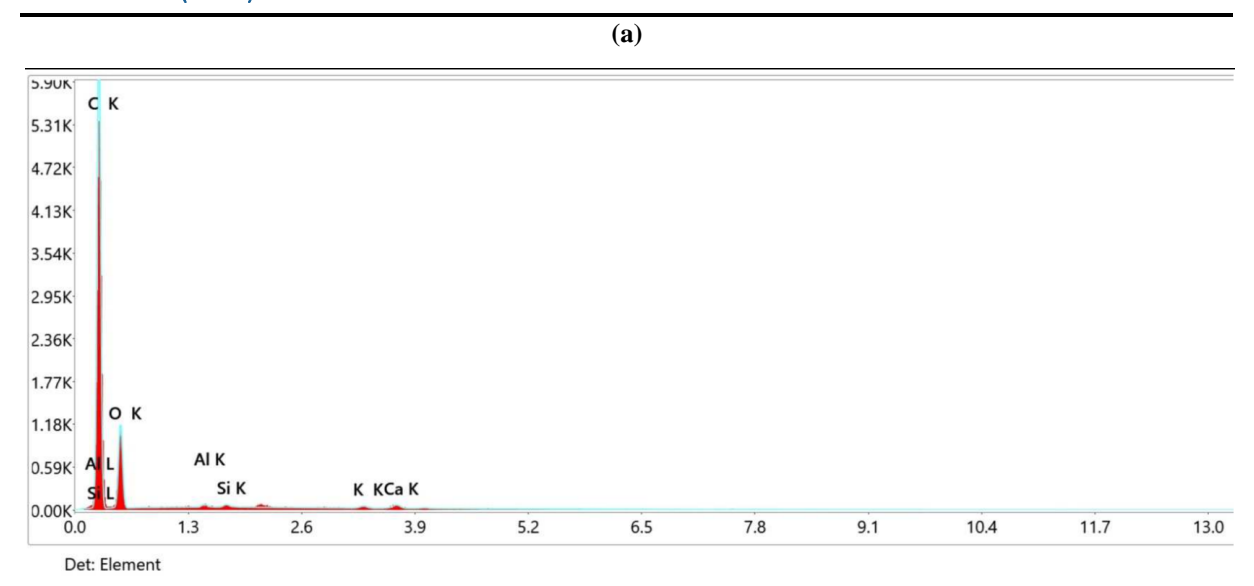
Pyrolysis	KOH-activated		
Pore diameter	Unit	Pore diameter	Unit
2.839	μm	2.137	μm
25.29	μm	1.217	μm
268.7	nm	1.452	μm
612.6	nm	1.560	μm
339.8	nm	1.702	μm
404.8	nm		
509.8	nm		
350.9	nm		
445.8	nm		
321.9	nm		

EDX ANALYSIS

SEM technique combined with EDX can identify the elements from the phase seen in the microstructure image. ⁴⁰ Analysis of EDX spectra of pyrolyzed and KOH-activated walnut shell carbon (Figure-4). Table-3 shows that the amount of photoelectron kinetic energy of each element is different. The photoelectron kinetic energy graph of pyrolyzed walnut shell carbon can be seen in Figure-5 (a, b, c). At the same time, the photoelectron kinetic energy graph of KOH-activated walnut shell carbon can be seen in Figure-5 (d, e, f). The photoelectron kinetic energy of pyrolyzed and KOH-activated walnut shell carbon is the same. Element C has a small photoelectron kinetic energy of 0.277 keV, while element Ca has the highest photoelectron kinetic energy of 3.692 keV.

ISSN: 1001-4055

Vol. 45 No. 2 (2024)



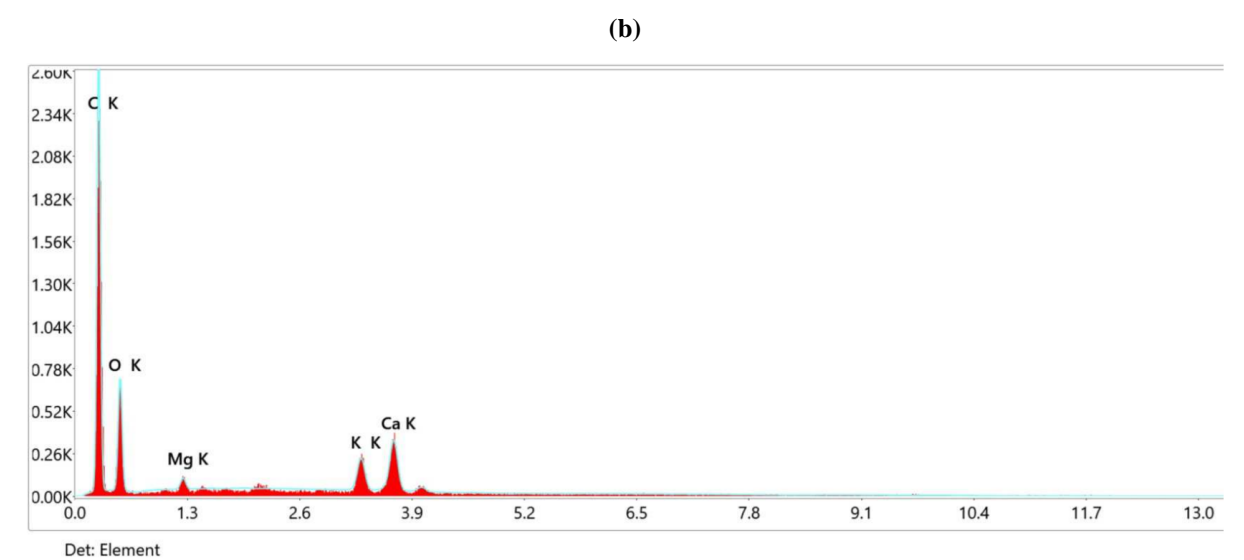


Fig.-4: EDX Spectra of Pyrolyzed (a) and KOH-Activated Walnut Shell Carbon.

Table-3: EDX Analysis Results of Pyrolyzed and KOH-Activated Walnut Shell Carbon.

No		Pyrolyzed	d	KOH-activated			
	Eleme	Photoelectron	Mass	Atoms	Photoelektron	Mass	Atoms
	nts	KE (keV)	(%)	(%)	KE (keV)	(%)	(%)
1	С	0.277	70.60	78.20	0.277	79.40	83.80
2	O	0.525	24.10	20.00	0.525	20.10	16.00
3	Mg	1.254	0.30	0.20	1.254	0.00	0.00
4	Al	1.486	0.00	0.00	1.486	0.10	0.00
5	Si	1.740	0.00	0.00	1.740	0.10	0.00
6	K	3.314	1.60	0.60	3.314	0.10	0.00
7	Ca	3.692	3.30	1.10	3.692	0.20	0.10
7	Γotal	12.288	99.90	99.90	12.288	100.0	99.90

Karakteristik energi kinetik fotoelektron dari unsur karbon hasil pirolisis dan karbon hasil aktivasi KOH adalah sama, sedangkan persen (%) massa dan persen (%) atom masing-masing unsur berbeda²⁸.

.

ISSN: 1001-4055

Vol. 45 No. 2 (2024)

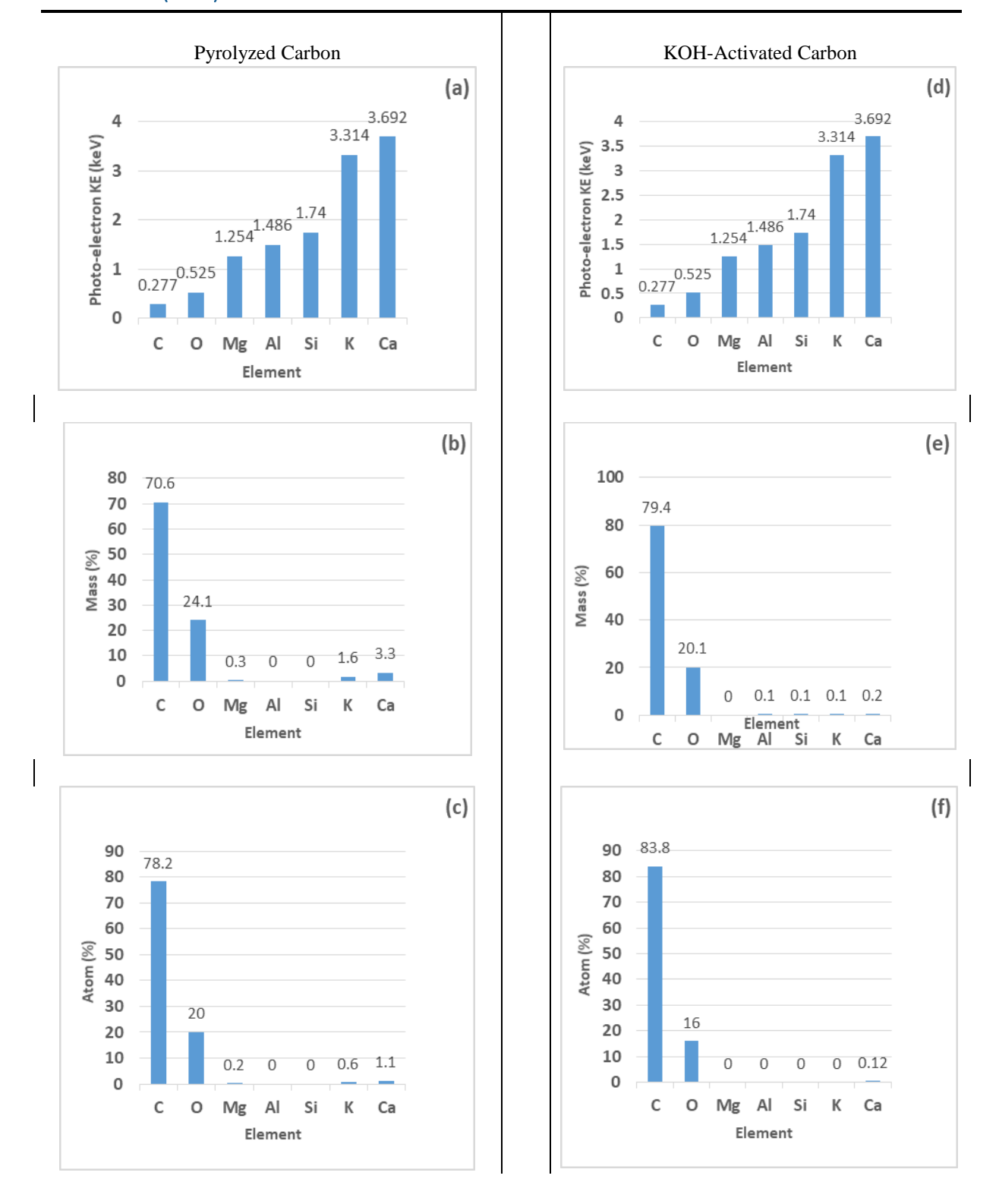


Fig.-5. Graphs of (a and d) KE Photo Electron, (b and e) Mass %, (c and f) Aomic % of Pyrolyzed and KOH-Activated Walnut Shell Carbon.

The percent mass and C atoms from the pyrolyzed were 70.60 and 78.20%, respectively. While, for the KOH-activated one is 79.40% and 83.80%. The presences of O, Mg, Al, Si, K, and Ca indicate an incomplete pyrolysis or carbonization process. The increase in carbon content in each carbons is associated with an increase in the number of pores. While the increase in pore diameter is due to the loss of impurities, namely O, Mg,

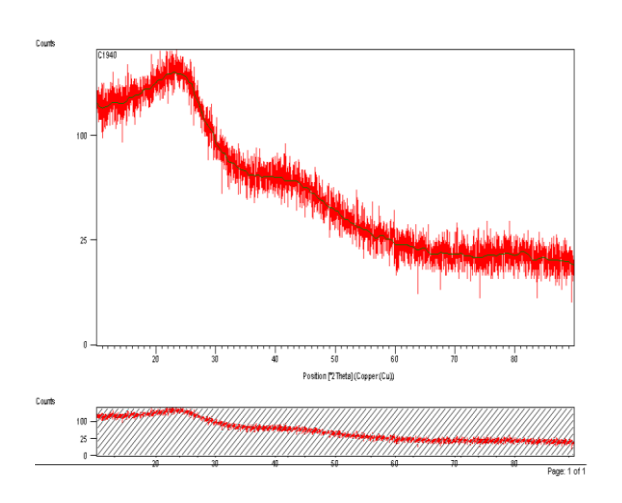
ISSN: 1001-4055

Vol. 45 No. 2 (2024)

Al, Si, K, and Ca, which are also in accordance with the decrease in impurity. The increase in pore diameter indicates that the walnut shell carbon is purer after activation with the KOH activator.

XRD ANALYSIS

XRD analysis was conducted to identify the sample's crystal phase, crystal structure, and crystallinity.⁴³ In the XRD characterization, observed diffractograms of pyrolyzed and KOH-activated walnut shell carbon samples are shown in Figure-6 and Figure-7, respectively. Figure 6 shows a broad diffraction background, irregular background intensity, and the absence of sharp peaks, revealing a highly amorphous structure.^{30, 43} The KOH-activated walnut shell carbon peaks showed 2Θ peaks of 27.7509° and 29.3071° . The scattering of crystallinity in the KOH-activated shell carbon is higher than the pyrolyzed one. The profile of carbon after KOH activation looks simple and only shows two broad diffraction bands in the 2Θ angle range, namely 27.7509° and 29.3071° , almost the same as the results of research from Gisgis et al.⁴⁴, which peak $2\Theta = 23-30^{\circ}$ and $43-48^{\circ}$.



Curb 225 - (1942)

111 - (1942)

112 - (1942)

113 - (1942)

114 - (1942)

115 - (1942)

116 - (1942)

117 - (1942)

118 - (1942)

119 - (1942)

119 - (1942)

119 - (1942)

119 - (1942)

119 - (1942)

119 - (1942)

119 - (1942)

119 - (1942)

119 - (1942)

119 - (1942)

119 - (1942)

119 - (1942)

119 - (1942)

119 - (1942)

119 - (1942)

119 - (1942)

119 - (1942)

119 - (1942)

119 - (1942)

119 - (1942)

119 - (1942)

119 - (1942)

119 - (1942)

119 - (1942)

119 - (1942)

119 - (1942)

119 - (1942)

119 - (1942)

119 - (1942)

119 - (1942)

119 - (1942)

119 - (1942)

119 - (1942)

119 - (1942)

119 - (1942)

119 - (1942)

119 - (1942)

119 - (1942)

119 - (1942)

119 - (1942)

119 - (1942)

119 - (1942)

119 - (1942)

119 - (1942)

119 - (1942)

119 - (1942)

119 - (1942)

119 - (1942)

119 - (1942)

119 - (1942)

119 - (1942)

119 - (1942)

119 - (1942)

119 - (1942)

119 - (1942)

119 - (1942)

119 - (1942)

119 - (1942)

119 - (1942)

119 - (1942)

119 - (1942)

119 - (1942)

119 - (1942)

119 - (1942)

119 - (1942)

119 - (1942)

119 - (1942)

119 - (1942)

119 - (1942)

119 - (1942)

119 - (1942)

119 - (1942)

119 - (1942)

119 - (1942)

119 - (1942)

119 - (1942)

119 - (1942)

119 - (1942)

119 - (1942)

119 - (1942)

119 - (1942)

119 - (1942)

119 - (1942)

119 - (1942)

119 - (1942)

119 - (1942)

119 - (1942)

119 - (1942)

119 - (1942)

119 - (1942)

119 - (1942)

119 - (1942)

119 - (1942)

119 - (1942)

119 - (1942)

119 - (1942)

119 - (1942)

119 - (1942)

119 - (1942)

119 - (1942)

119 - (1942)

119 - (1942)

119 - (1942)

119 - (1942)

119 - (1942)

119 - (1942)

119 - (1942)

119 - (1942)

119 - (1942)

119 - (1942)

119 - (1942)

119 - (1942)

119 - (1942)

119 - (1942)

119 - (1942)

119 - (1942)

119 - (1942)

119 - (1942)

119 - (1942)

119 - (1942)

119 - (1942)

119 - (1942)

119 - (1942)

119 - (1942)

119 - (1942)

119 - (1942)

119 - (1942)

119 - (1942)

119 - (1942)

119 - (1942)

119 - (1942)

119 - (1942)

119 - (1942)

119 - (1942)

119 - (1942)

119 - (1942)

119 - (1942

Fig.-6: Diffractogram of Pyrolyzed Walnut Shell Carbon.

Fig.-7: Diffractogram of KOH-Activated Walnut Shell Carbon

CONCLUSION

The results of FTIR analysis showed that carbon has functional groups of C-H aromatic, C-H aliphatic, C-O alcohol, C-O carboxylic acid, and C-O esters. Pore diameter of walnut shell carbon from pyrolysis ranged from 339.8 nm to 2,839 μ m and pore diameter of walnut shell carbon after KOH activation ranged from 1,217 μ m to 2,137 μ m. SEM morphology shows that the surface structure of carbon particles from pyrolysis and carbon after KOH activation are inhomogeneous. The mass percent and atomic percent of carbon from walnut shell carbon from pyrolysis are 70.60% and 78.20%, while walnut shell carbon after KOH activation is 79.40% and 83.80%. The chemical activation process with the KOH activator can enlarge the carbon pores, increase carbon composition, and reduce the composition of minor elements contained in the walnut shell carbon. The XRD diffractogram shows that the pyrolyzed walnut shell carbon has a dense peak and relatively low intensity compared to the walnut shell carbon after KOH activation, which shows a denser peak and relatively higher intensity. The appearance of diffractograms with broad diffraction, irregular diffraction intensity, and the absence of sharp peaks revealed the structure of both carbons to be highly amorphous.

ACKNOWLEDGMENTS

The authors would like to thank the chairman of the Institute for Research and Community Service of Manado State University for financial support for the publication of this article.

CONFLICT OF INTERESTS

The authors declare that there is no conflict of interest.

ISSN: 1001-4055 Vol. 45 No. 2 (2024)

AUTHOR CONTRIBUTIONS

All the authors contributed significantly to this manuscript, participated in reviewing it, and approved the final draft for publication.

REFERENCE

- Tapia, M. I., Sánchez-Morgado, J. R., García-Parra, J., Ramírez, R., Hernández, T., González-Gómez, D. (2013). Conparative study of the nutritional and bioactive compounds content of four walnut (juglans regia L.) cultivars. J. of food composition and analysis, 31(2), 232–237. (https://doi.org/101016/j.jfca.2013.06.004)
- 2. Yang, J., Qiu, K. (2010). Preparation of activated carbons from walnut shells via vacuum chemical activation for methylene blue removal. Chem. eng. j. 165(1), 209–217. (DOI:10.1016/J.CE.J.2010.09.019).
- 3. Sharahi, M., Hivechi, A., Bahrami, S. H., Hemmatinejad, N., Milan, P. B. (2021). Co-electrospinning of lignocellulosic nanoparticles sunthesized from walnut shells with poly(caprolactone) and gelatin for tissue engineering applications. Cellulose, 28(8), 4943–4957. (DOI: 10.1007/s10570-021-03709-w)
- 4. A. Spagnoli, D. A. Giannakoudakis, S. Bashkova, Adsorption of methylene blue on cashew nut shell based carbons activated with zinc chloride: The role of surface and structural parameters, J. of melecular liquids, 229 (2017) 465-471. (https://doi.org/10.16/j.molliq.2016.12.106)
- Yusnaini, Suryanto, E., Hasan, S., Wulansari, A., Dewi, W. K. (2021). The characteristics of volatile compounds of kenari (Canarium indicum L.) shell liquid smoke, 7th International conference on sustainable agriculture, food and energy, IOP conf. series: earth and environ. Sci., 709, 1-10. . (doi:10.1088/1755-1315/709/1/012032)
- Olive, B. O. S., Fabien, B. E., Edwige, M. A., Anicet, N. P. M., Ateba, A. (2021). Physico-chemical and thermal characterization of canarium schweinfurthii engl (Cs) shells. SSRG Int. J. of mat. sci. and eng., 7(3), 9-15. (http://creativecommons.org/licenses/by-nc-cd/4.0/), ISSN: 2394-8884/doi:10.14445/23948884/IJMSE-V713P102.
- 7. Maguie, K. A., Nsami, N. J., Daouda, K., Nangah, C. R., Desire, B. P., Odogu, A. P., Z. Z., Bertrand, Mbadcam, K. J. (2017). Actived carbon based canarium scheweinfurthii shells for the removalof nitrate ions from aqueous solution. Int. j. of eng. sci. & res. tech., 7(7), 805-815. (http://www.ijesrt.com)
- 8. K. Acikalin, F. Karaca, Fexed-bed pyrolysis of walnut shell: Parameter effects on yields and characterization of products. J. of Analytical and Applied Pyrolysis, 125 (2017) 234-242. (https://doi.org/10.1016/j.jaap.2017.03.018).
- 9. Anom, I D. K. (2021). Kinetic study of gas formation in styrofoam pyrolysis. Acta chemica asiana, 4(2), 135-140. (DOI: 10.29303/aca.v4i2.76)
- 10. N. A. Rashidi, S. Yusup, A review on recent technological advancement in the activated carbon production from oil palm waste, Chem. engineering J., 314 (2017) 277-290. (https://doi.org/10.1016/j.cej.2016.11.059)
- 11. S. Wong, N. Ngadi, I. M. Inuwa, Recent advances in applications of activated carbon from biowaste for wastewater treatment: Ashort review. J. of cleaner production, 175 (2018) 361-375. (https://doi.org/10.1016/j.jclepro.2017.12.059)
- 12. X. Li, J. Qiu, Y. Hu, X. Ren, L. He, N. Zhao, T. Ye, X. Zhao, Characterization and comparison of walnut shells-based activated carbons and their adsorptive properties, Adsorption Science Technology, 38(9-10) (2020) 450-463. (DOI: 10.1177.0263617420946524)
- 13. Wang, L., Guo, Y., Zou, B., Rong, C., Ma, X., Y. Qu, Y., Wang, Z. (2011). High surface area porous carbons prepared from hydrochars by phosphoric acid activation. Biores. tech., 102(2), 1947-1950. (https://doi.org/10.1016/j.biortech.2010.08.100)

- 14. X. Zhang, B. Gao, J. Fang, W. Zou, L. Dong, C. Cao, J. Zhang, Y. Li, H. Wang, Chemically actived hydrochar as an effective adsorbent for volatile organic compounds (VOCs), Chemosphere, 218 (2019) 680-686. (https://doi.org/10.1016/j.chemosphere.2018.11.144)
- 15. Raymundo-Pinero, E., Azais, P., Cacciaguerra, T., Cazorla-Amoros, D. (2005). KOH and NaOH activation mechanisms of multiwalled carbon nanotubes with different structural organization. Carbon, 43, 786-795. (https://doi.org/10.1016/j.carbon.2004.11.005)
- X. Qiu, L. Wang, H. Zhu, Lightweight and efficient mocrowave absorbing materials based on walnut shell-derived nano-porous carbon, Nanoscale, 9(22) (2017) 7408-7418. (https://doi.org./10.1039/rsc crossmark_policy)
- 17. Prayogatama, a., Nuryoto, Kurniawan, T. (2022). Modifikasi karbon aktif dengan aktivasi kimia dan fisika menjadi elektroda superkapasitor. J. sains dan tek., 11(1), 47-58. (https://dx.doi.org/10.23887/jst-undiksha.v11i1.4284)
- 18. Q. Yu, M. Li, P. Ning, H. Yi, X. Tang, Preparation and phosphine adsorption of activated carbon prepared from walnut shells by KOH chemical activation, Separation science and technology, 49(15) (2014) 2366-2375. (https://doi.org/10.1080/01496395.2014.917326)
- 19. J. Liu, B. Liu, B. Wang, Z. Huang, L. Hu, X. Ke, L. Liu, Z. Shi, Z. Guo, Walnut shell-derived activated carbon: Synthesis and its application in the sulfur cathode for lithium-sulfur batteries, J. of alloys and compounds, 718 (2017) 373-378.(https://doi.org/10.1016/j.jallcom.2017.05.206)
- 20. Z. Alimohammadi, H. Younessi, N. Bahramifar, Desorption reactive red 198 from activated carbon prepared from walnut shell: Effects of temperature, sodium carbonate concentration and organic solvent dose, Advenced environmental technology, 3 (2016) 137-141. (doi.10.22104/AET.2017.432)
- 21. Jamilatun, S., Salamah, S., Isparulita, I. D. (2016). Karakteristik karbon aktif dari tempurung kelapa dengan pengaktivasi H₂SO₄, CHEMICA: J. tek. kim. 2(1), 13. (DOI: 10.26555/chemica.v2i1.4562)
- 22. Merin, P., Jimmy Joy, P., Muralidharan, M. N., Veena Gopalan, E., Seema, A. (2021). Biomass-derived activated carbon for High-performance supercapacitor electrode applications. Chem. eng. tech., 44(5), 844–851. (https://doi.org/10.1002/ceat.202000450)
- 23. G. P. Garcia, Activated carbon from lignocellulosics precursors: A review of the synthesis methods, characterization techniques and applications', Renewable and sustainable energy reviews, 82 (2018) 1393-1414. (https://doi.org/10.1016/j.rser.2017.04.117)
- 24. Darmawan, S. Syafii, W., Wistara, W. J., Maddu, A., Pari, G. (2015). Kajian arang pirolisis, arang-hidro dan karbon aktif dari kayu Acacia mangium Willd. Menggunakan difraksi sinar-x (X-Ray diffraction observation of pyrolized-char, hydro-car and activated carbon made of Acacia mangium Willd. Wood. J. penel. hasil hutan. 33(2), 81-92. (DOI: 10.20886/jphh.2015.33.2.81-92)
- 25. Munasir, Triwikantoro, Zainuri, Darminto. (2012). Uji XRD dan XRF pada bahan mineral (batuan dan pasir) sebagai sumber material cerdas (CaCO3 dan SiO2). J. penel. fisika dan aplikasinya (JPFA), 2(1), 20-29. (https://doi.org/10.26740/jpfa.v2n1.p20-29)
- 26. Rampe, M. J., Santoso, I. R. S., Rampe, H. L., Tiwow, V. A., Rorano, T. E. A. (2022). Study of pore and chemical composition of charcoal shell in Bolaang Mongondow, Sulawesi, Indonesia. Karbala int. j. of modern sci. 8(1), 96-104. (https://doi.org/10.33640/2405-609X3208)
- 27. Wibowo, S., Syafi, W., Pari, G. (2011). Karakterisasi permukaan arang aktif tempurung biji nyamplung. Makara, teknol., 15, 17-24. (DOI: 10.7454/mst.v15i1.852)
- 28. Wijaya, D. R. P., Martono, Y., Riyanto, C. A. (2018). Synthesis and characterization of nano activated carbon tea waste (Camellia sinensis L.) viewed from the content and ratio of orthophosphoric acid. Int. j. of chem. res., 3(2), 49-58. (https://doi.org/10.20885/ijcr.vol3.iss2.art2)

- 29. Sahoo, S. Ramgopal, M. (2016). Experimental studies on an indigenous coconut shell based actived carbon suitable for natural gas storaga. Sadhana, 41(4), 459-468. (DOI: 10.1007//s12046-016-0483-X).
- 30. S. G. Lu, S. Q. Bai, L. Zhu, H. D. Shan, Removal mechanism of posphate from aqueous solution by fly ash, J. of hazardous materials, 161 (2009) 95-101. (https://doi.org/10.1016/j.jhazmat.2008.02.123)
- 31. Lee, K. C., Lim, M. S. W., Hong, Z. Y., Chong, S., Tiong, T. J., Pan, G. T., Huang, C. M. (2021). Coconut shell-derived activated carbon for high-performance solid-state supercapacitors. Energies, 14, 4546. (https://doi.org/10.3390/en14154546)
- 32. Efeovbokhan, V. E., Alagbe, E. E., Odika, B., Babalola, R., Oladimeji, T. E., Abatan, O. G., Yusuf, E. O. (2019). Preparation and characterization of activated carbon from plantain peel and coconut shell using biological activators. J. phys. conf., 1378, 032035. (DOI: 10.1088/1742-6596/1378/3/03203)
- 33. Song, C., Wu, S., Cheng, M., Tao, P., Shao, M., Gao, G. (2014). Adsorption studies of coconut shell carbons prepared by KOH activation for removal of lead(II) from aqueous solutions. Sustainability, 6, 86-98. (https://doi.org/10.3390/su6010086).
- 34. Prauchner, M. J., Reinoso, F. R. (2012). Chemical versus physical activation of coconut shell: a comparative study. Microporous Mesoporous Mater, 152, 163-171. (https://doi.org/10.1016/j.micromeso.2011.11.040)
- 35. Anom, I D. K., Lombok, J. Z. (2022). Reaction kinetics in pyrolysis og human waste. Acta chimica asiana, 5(1), 186-192. (DOI: 10.29303/aca.v5i1.113)
- 36. Shaheed, R., Azhari, C. H., Ahsan, A., Mohtar, W. H. M. W. (2015). Production and characterization of low-tech activated carbon from coconut shell, J. hydrol. environ. Rs., 3(1), 1-14. (https://hdl.handle.net/10652/4505)
- 37. Huang, P. H., Cheng, H. H., Lin, S. H. (2015). Adsoption of carbon dioxide onto actived carbon prepared from coconut shell. J. chem., 106590. (https://doi.org/10.1155/2015/106590)
- 38. Manurung, M. Bukit, N. (2020). Pembuatan carbon black dari tempurung kelapa menggunakan ball mill dan metode kopresipitasi. J. einstein (e-Journal), 8(2), 1-7. (DOI: https://doi.org/10.2411/einstein.v8i2.14223)
- 39. Duan, X., Srinivasakannan, C., Yang, K., Peng, J., Zhang, L. (2012). Effects of heating method and activating agent on the porous structure of activated carbons from coconut shell. Waste biomass valor, 3, 131-139. (DOI:101007/s12649-011-9097-z).
- 40. Islam, M. S., Ang, B. C., Gharehkhan, S., Afifi, A. B. M. (2016). Adsorption capability of activated carbon synthesized from coconut shell. Carbon lett. 20, 1-9. (DOI:10.5714/CL.2016.20.001)
- 41. Hartini, Hidayat, Y. Mudjijono. (2015). Study pore characterization of γ-alumina-activated carbon composite made of Cassava peels (Manihot esculenta Cranz). ALCHEMY, 11, 47-57. (http://.doi.org/10.20961/alchemy.11.1.106.47)
- 42. Demiral, H., Hakan, D., Demiral, I. (2008). Pore structure of actived carbon prepared from hazelnut bagasse by chemical activation. Surf. interface anal., 40, 616-619. (https://doi.org/10.1002/sia.2631)
- Shrestha, L. K., Adhikari, L., Shrestha, R. G., Adhikari, M. P., Adhikari, R., Hill, J. P., Pradhananga, R. R., Ariga, K. (2016). Nanoporous carbon materials with enhanced supercapacitance performanc and non-aromatic chemical sensing with C1/C2 alcohol discrimination. Sci. and tech. of advanced materials, 17(1), 483-492 (doi:10.1080/14686996.2016.1219971)
- 44. Girgis, B. S., Temerk, Y. M., Gadelrab, M. M., Abdullah, I. D. (2007). X-ray diffraction patterns of activated carbons prepared under various conditions. Cancon lett, 8, 95-100. (DOI: 10.5714/CL.2007.8.2.095)